

COMPUTER MODELLING OF RADIATION- INDUCED PROCESSES IN OXIDE SOLIDS

E.A. KOTOMIN,

V.N. KUZOVKOV, A.I. POPOV,
D. GRYAZNOV, A. PLATONENKO



*Institute of Solid State Physics,
University of Latvia, Riga, Latvia*

In memory of Cheslav Lushchik (15.02.1928-08.08.2020)



The radiation-resistant oxide insulators (Al_2O_3 , $\text{Y}_3\text{Al}_5\text{O}_{12}$, MgAl_2O_4) are important materials for application in fusion reactors, e.g. as optical windows. It is very important to predict/simulate a long-time defect structure evolution including thermal defect annealing after irradiation. Defect aggregation, accumulation or recombination occurs due to diffusion controlled reactions between mobile defects. Thus, for further prediction of the radiation stability of materials, it is necessary to determine main kinetic parameters of basic point defects characterized by the migration energy E_a and diffusion pre-exponent D_0 .

Despite the well studied F-type centers (anion vacancies with trapped electrons), the structure and mobility of complementary defects – **interstitial anions** – are poorly studied, due to lack of optical absorption, ESR and Raman measurements. It is well known that interstitials are much more mobile than the F-type centers and thus control many properties of irradiated solids.

In this talk, we discuss the latest results of the defect computer simulations combining the first principles calculation of the atomic, electronic, magnetic structure and optical properties of above mentioned defective oxides with the kinetics of defect diffusion-controlled recombination upon annealing.

Primary radiation defects in ionic solids consist of **Frenkel defects** —pairs of anion vacancies with trapped electrons (*F*-type centers) and interstitial ions. Their thermal annealing is controlled by the interstitial ion migration, whose mobility is much higher than that of the *F* centers. The basic theory (how to extract from experimental data the *migration energy* of interstitials and *pre-exponential factor* of diffusion) was developed and applied to irradiated insulators in our recent papers:

- V.Kuzovkov, E.Kotomin, A.Popov, R.Villa, Nucl. Inst. Meth. **B 374**, 107 (2016).
E.Kotomin, V.Kuzovkov, A.Popov, J.Maier, R.Vila, J.Phys.Chem.A, **22**, 28 (2018).

Traditionally, it is assumed in kinetics of defect recombination that defect diffusion is defined uniquely by the two independent parameters – the migration energy E_a and pre-exponential factor D_0 . However, this is true only at low defect concentrations.

As we have shown, these parameters depend on the radiation fluence. Moreover, there is a clear correlation of these two parameters which satisfies the so-called Meyer–Neldel rule (MNR). This rule observed more than once earlier in glasses, liquids, and disordered materials, but not in the irradiated materials.

We analyze here the available experimental kinetics of the *F*-type electronic and *V*-type hole center annealing for two wide gap insulating materials with different crystalline structures:

neutron/ion-irradiated Al_2O_3 (sapphire)

V.Kuzovkov, E.Kotomin, A.Popov, R.Villa, Nucl. Inst. Meth. **B 374**, 107 (2016).

E.Kotomin, V.Kuzovkov, A.Popov, J.Maier, R.Vila, J.Phys.Chem.A, **22**, 28 (2018).

A.Platonenko, D. Gryaznov, Yu.Zhukovskii, E.A. Kotomin, Nucl. Inst. Meth. **B 435**, 74 (2018),

and MgAl_2O_4 spinel:

A.Platonenko, D.Gryaznov, Yu. Zhukovskii, E.A. Kotomin, Phys Stat Sol B **256**, 1800282 (2019)

A.Lushchik, E.A.Kotomin, A.i.Popov, V.Kuzovkov et al, Scientific Reports 10, 7810 (2020)

In this talk, we demonstrate that the dependence of defect migration parameters on the radiation fluence plays an important role in the quantitative analysis of the radiation damage of real materials and should not be neglected.

We performed multiscale computer modelling of radiation defects on a series of oxides, starting with first principles calculations of the atomic, electronic and magnetic structure of primary point defects, their migration barriers, and then the kinetics of their diffusion-controlled recombination upon annealing.

One of main previous theoretical predictions was that the interstitial oxygen atoms O_i (Frenkel defects) are unstable in the interstitial positions and form dumbbells with a regular O₂⁻ ions, similar to the V_K centers (self-trapped holes) in alkali halides.

The first dumbbell calculation was performed by us long ago in ionic MgO crystals:

T.Brudevoll, E.A.Kotomin, N.Christensen, Phys Rev B 53, 7731, 1996.

The migration is a combination of 111 jumps from one O₂⁻ site after breaking the bond, to the next one oxygen ion, with a periodic dumbbell rotations in sites

One of key problems: is O_i in Frenkel pair a neutral O atom or O⁻ ion? We modelled both cases.

Electronic/vibrational properties of defects in oxides

- Materials: YAG, Al_2O_3 , MgAl_2O_4
- Method: DFT and Gaussian basis set (LCAO)
- Accurate hybrid (e.g. HSE06) exchange-correlation functional
- Computer code: CRYSTAL17
- Supercell model, large scale computer simulations
- Direct method for the calculation of phonons
- Raman and IR vibrations were analyzed

Theoretical modelling of oxides

Large scale first principles calculations:

Oxygen interstitials were confirmed

in Al₂O₃, MgAl₂O₄ -> formation of dumbbell -> distance 1.44
(1.42 in spinel) Å,

Zhukovskii et al, NIM B 374, 29 (2016)

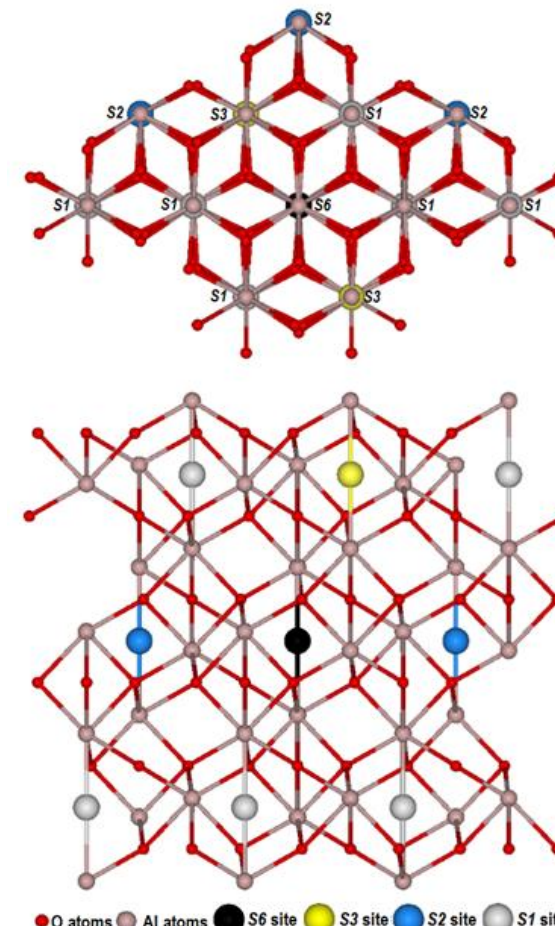
phonon frequency 1067 (1142 in spinel) cm⁻¹, formation
energy 3.99 eV (2.51 eV in spinel)

General theory of interstitials in oxides:

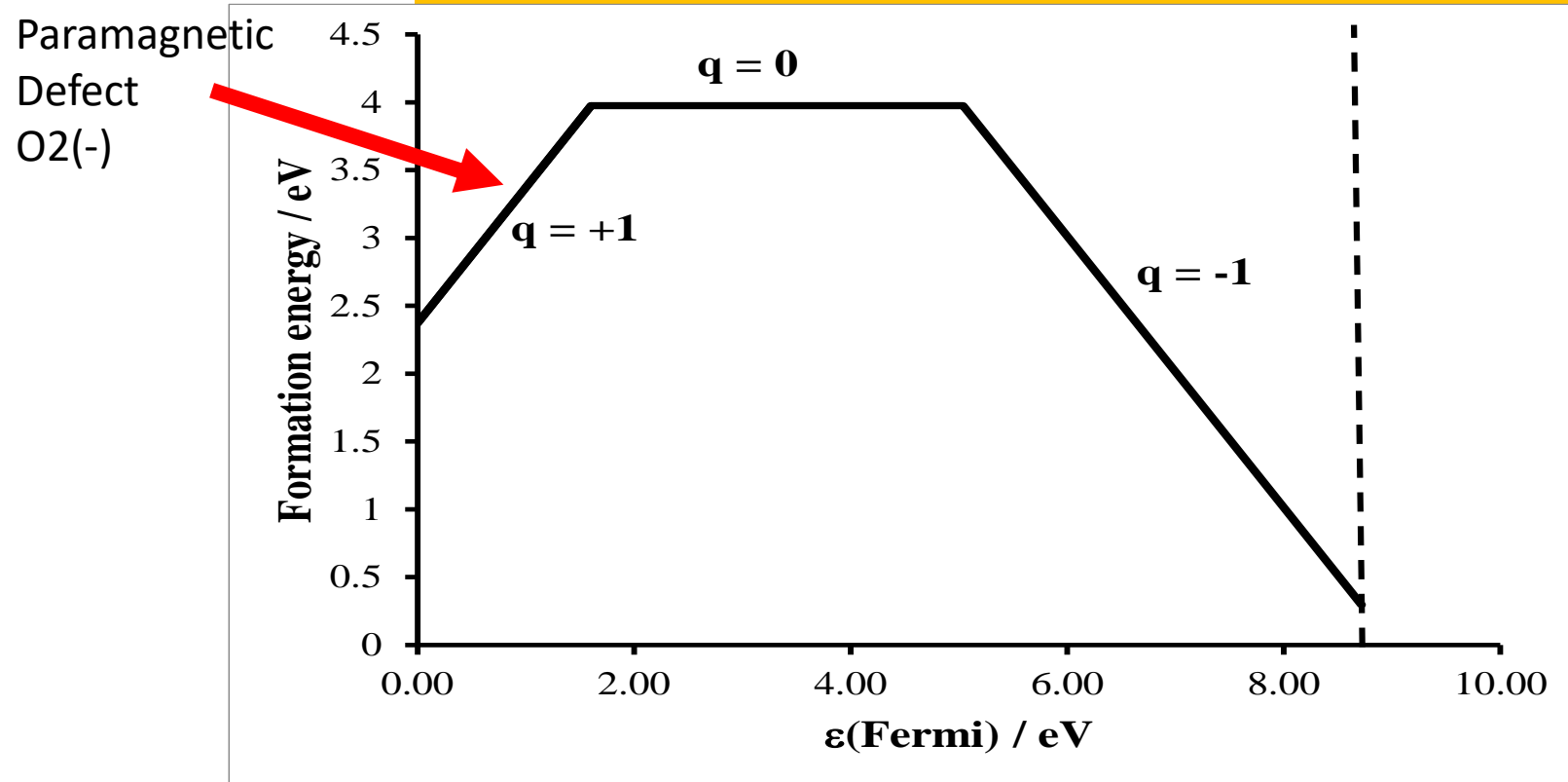
Evarestov et al. Comp. Mater. Sci. 2018, 150, 517

4 types of interstitial positions,
shown in colors here:

Symmetry analysis by Evarestov et al,
PCCP 19, 25245 (2017)



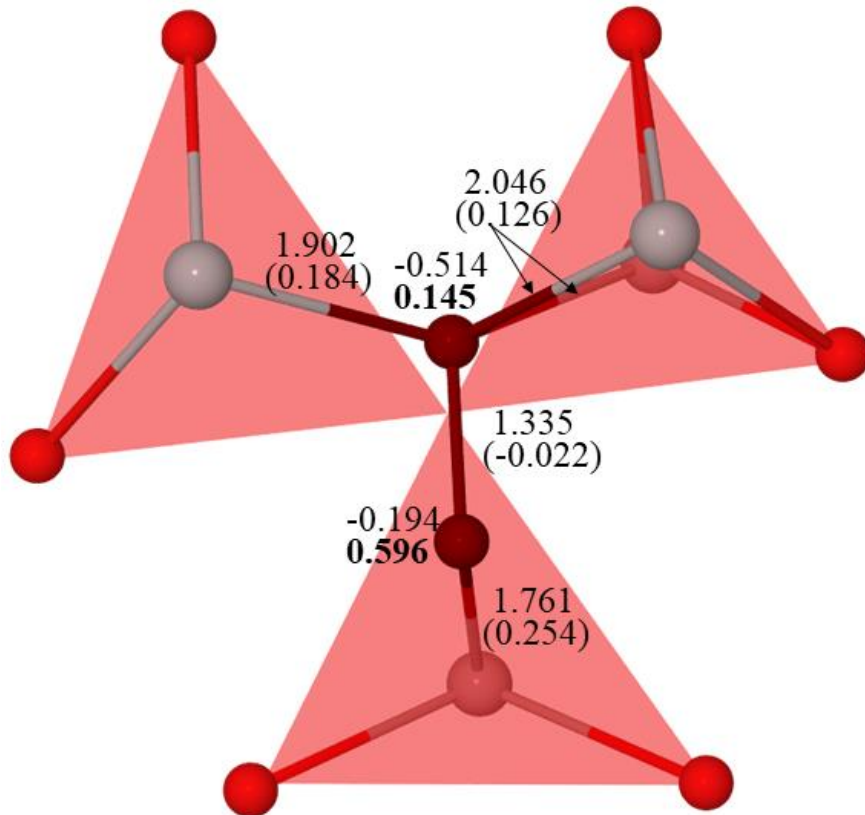
Three types of oxygen dumbbells were calculated, with net charges +1, 0, -1
Their formation energies depend on the Fermi energy position



Defect formation energy for O_2^- ($q = +1$, asymmetric configuration), O_2^{2-} ($q = 0$), O_2^{3-} ($q = -1$, pseudo-dumbbell configuration) as a function of the Fermi energy. The asymmetric configuration represents the ground state configuration shown in next figure. The dashed line shows the band gap value.

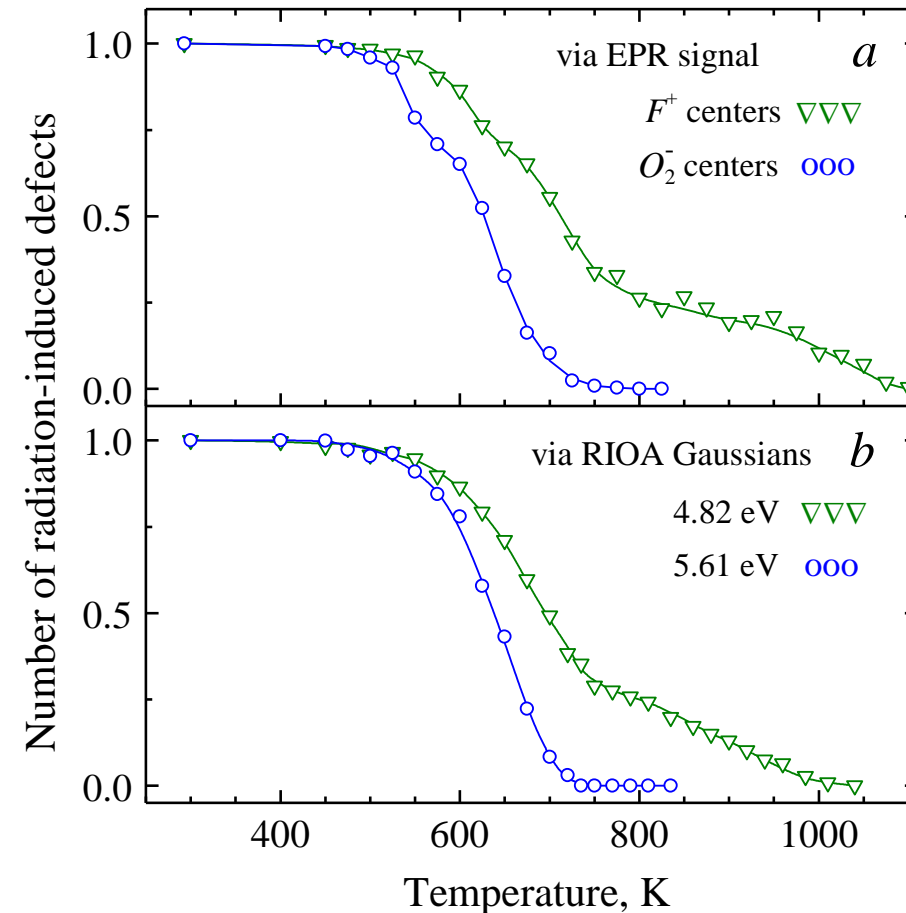
Superoxide defect O₂(-) (a hole trapped by neutral dumbbell) in corundum: dumbbell with q=1+

It was predicted theoretically and EPR-confirmed experimentally in Tartu (V.Seeman, A.Lushchik et al, Scientific Reports, 2020, in press). Bold numbers are atom spins, without bold - distances in Å, in brackets are bond populations (e) red atoms O, grey Al.



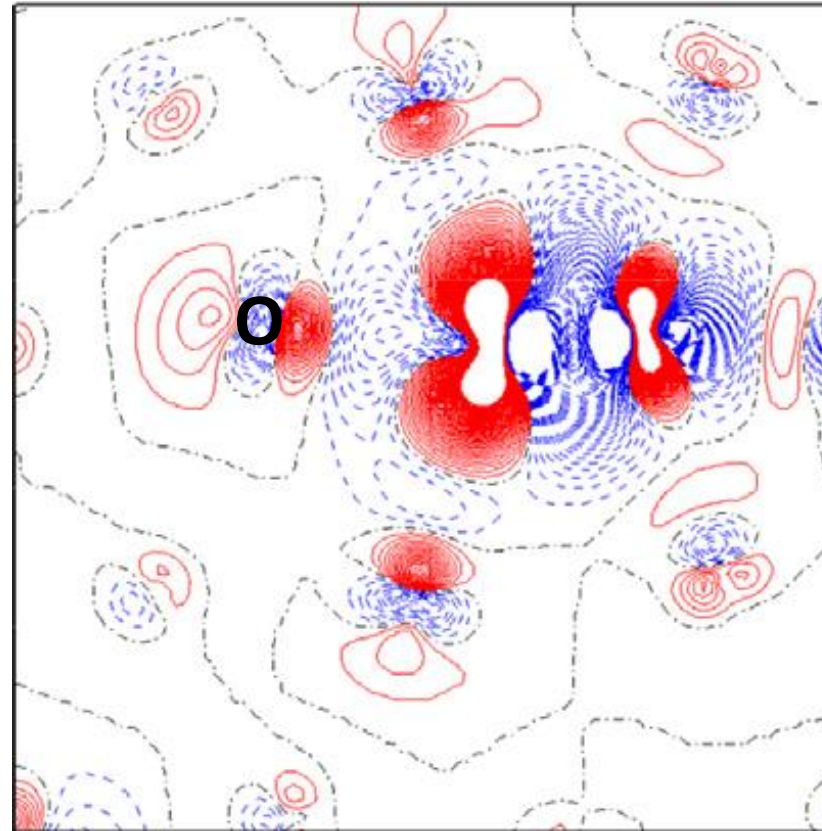
The annealing kinetics of the F+ and dumbbell defects

The delay with F+ recombination due to slow interstitial ion migration after dumbbell recombination



Electronic density distribution around dumbbell

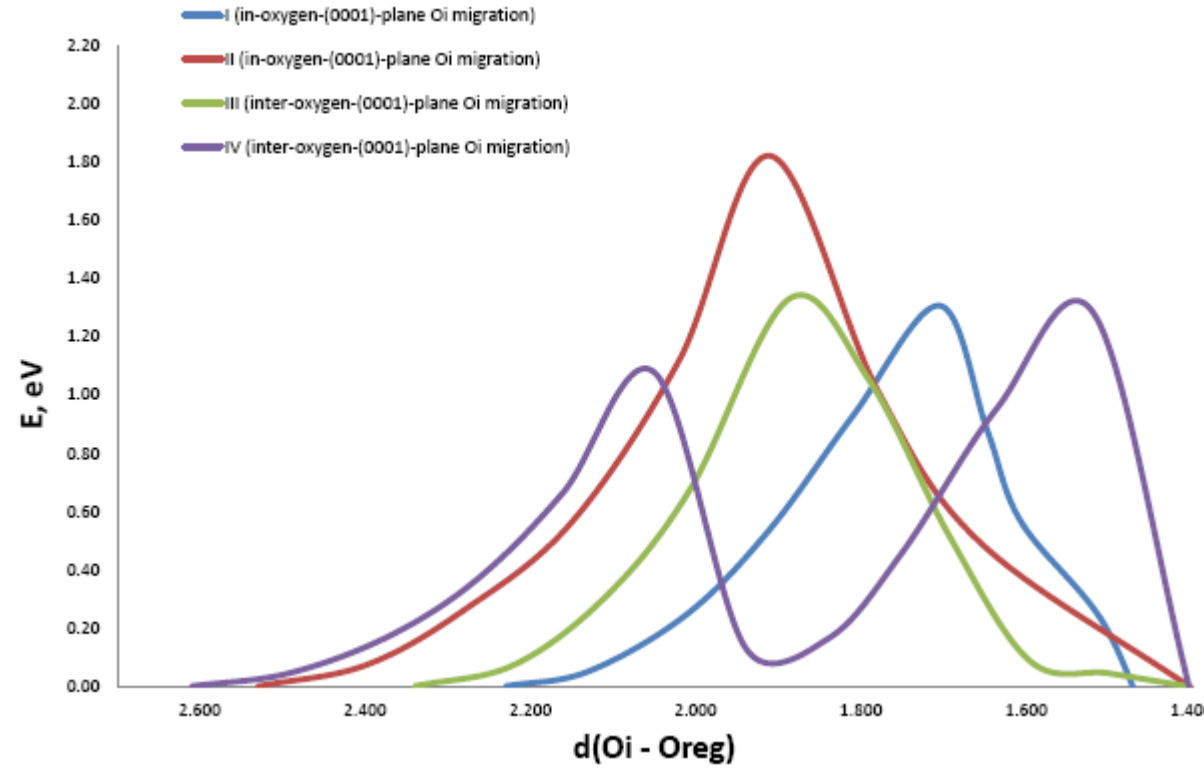
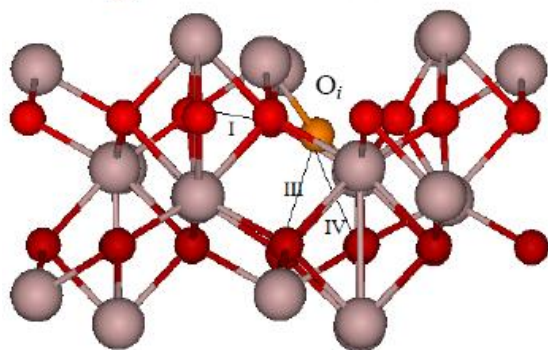
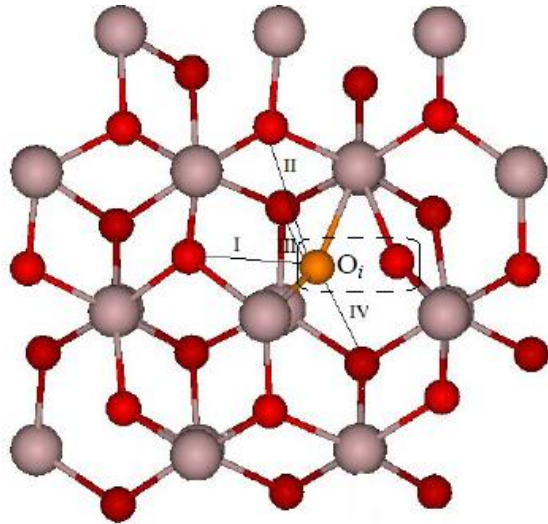
Blue color indicates electron
Density accumulation, red-
ist defiency



Interstitial oxygen migration paths and energy barrier estimation

Zhukovskii et al, NIM B 374, 29 (2016), Platonenko et al NIM B 435, 74 (2018)

4 migration paths for O_i(I, II, III, IV)



The migration energy for neutral O atom is 1.3 eV,
For charged interstitial smaller- 0.8 eV
Much smaller than for oxygen vacancy (4.5 eV)

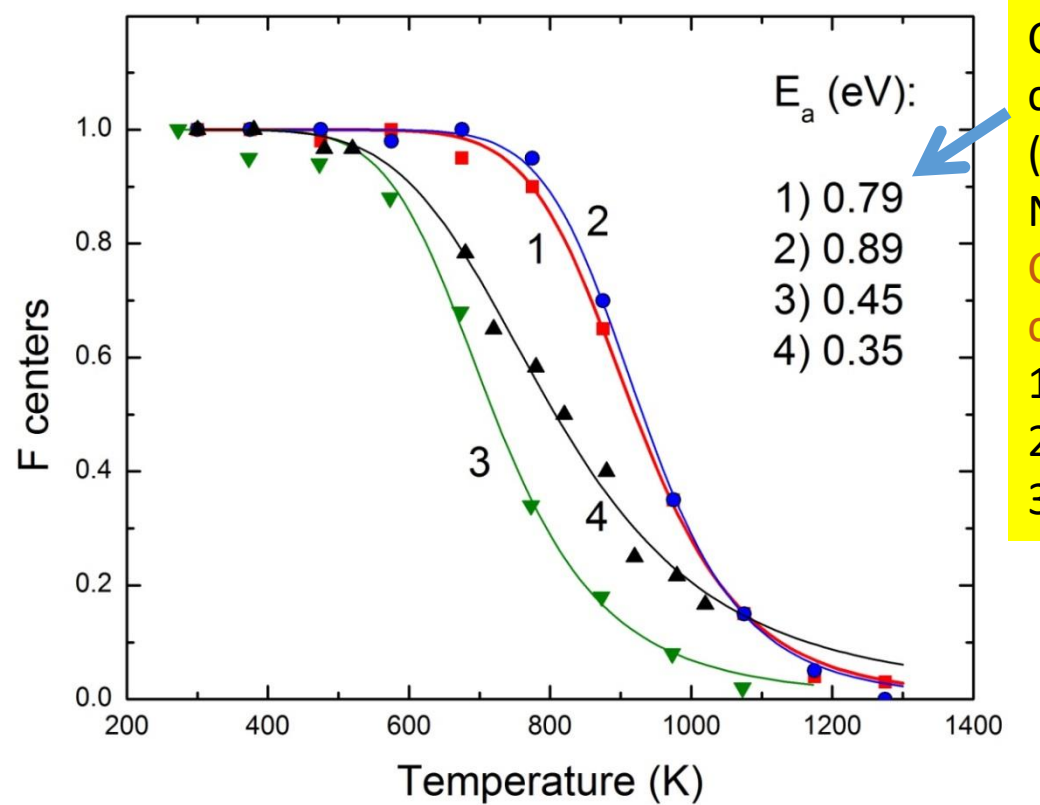
Despite numerous experimental data, very few theoretical efforts were devoted so far to the **quantitative** analysis of available kinetics, in order to extract main kinetic parameters- **interstitial** migration energy E_a and diffusion pre-exponent D_0 , necessary for further prediction of the secondary defect kinetics and radiation stability of sapphire and related materials. This was accompanied with *ab initio* calculations.

Our recent theory:

- ❖ E.A. Kotomin, V.N. Kuzovkov, A.I. Popov, J. Maier, R. Vila, *J. Phys Chem A* 122 (2018) 28;
- ❖ also *J. Nucl. Mater.* 502, 295 (2018);
- ❖ V.N. Kuzovkov, A.I. Popov, E.A. Kotomin et al, *Low Temp. Phys.*, **42**, 748 (2016).
 - defect creation, migration, interaction, recombination or colloid formation
 - diffusion-controlled bimolecular reactions
 - spatial correlation analysis through joint correlation functions

F-center recombination in neutron irradiated sapphire

Recombination of mobile interstitial O ions with immobile F centers :
very large dispersion of migration energies, likely due to different radiation fluences



Close to our *ab initio* calculations
(Platonenko et al,
NIM B 435, 74, 2018):
Choice between neutral and charged interstitials
1 Ramirez JAP 2007
2 Izerrouken NIM 2010
3 Bunch JACS 1974

The Meyer-Neldel rule (Phys.Zeits. 1937)

- The rule known in reaction kinetics, diffusion pre-exponent X:

$$\ln(X) = \ln(X_0) + E_a/k_B T_0 ,$$

where X_0 is a constant and T_0 some characteristic temperature

It could be also interpreted as the diffusion coefficient with exponentially dependent pre-exponent

$$D \sim \exp\left(\frac{E_a}{k_B T_0} - \frac{E_a}{k_B T}\right) , T < T_0$$

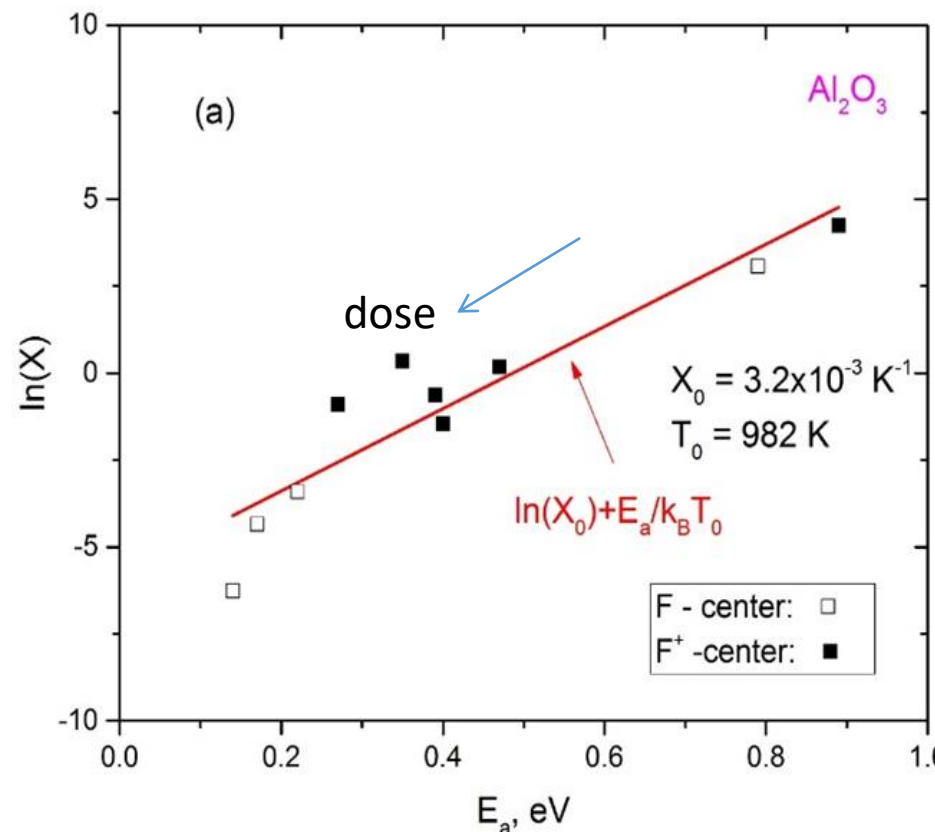
This relation was observed in many disordered systems in chemistry, biology, semiconductors

read more in: [Kotomin, Kuzovkov, Popov, J. Phys. Chem. A 122, 28 \(2018\)](#)

Correlation between E_a and pre-exponent X in corundum

(Popov et al, NIM B 433, 93 (2018))

Additional information – effect of radiation fluencies (dose)



10 orders of magnitude
in D_o , and factor of 5 in E_a !!

Similar effect was observed also
In MgF₂, MgO, spinel, YAG—
Kotomin et al, J Phys Chem A 122, 28 (2018) (see below)

Calculations of oxygen interstitials in MgAl₂O₄ spinel

Models: 3D defective: supercell models
With 56 and 112 atoms

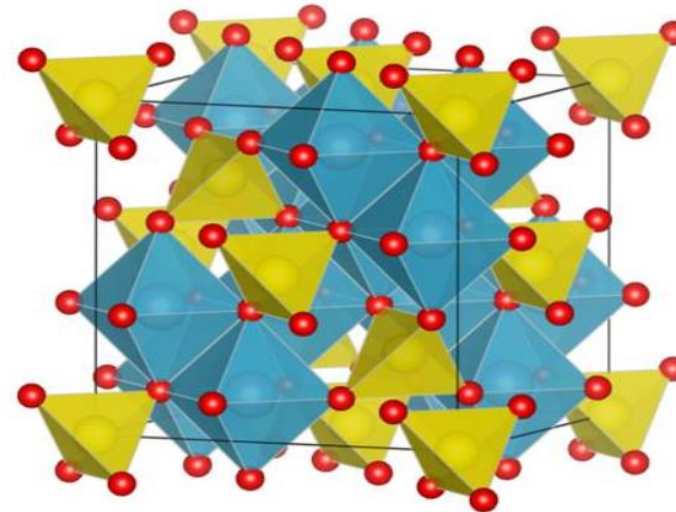
Code: An initio CRYSTAL14 (CRYSTAL17)
Hybrid HF-DFT: HSE06

Basis set: LCAO-GTO

Al: [Ne] 3s²3p
O: [6s-2111sp1d], Mg: [8s-511G]

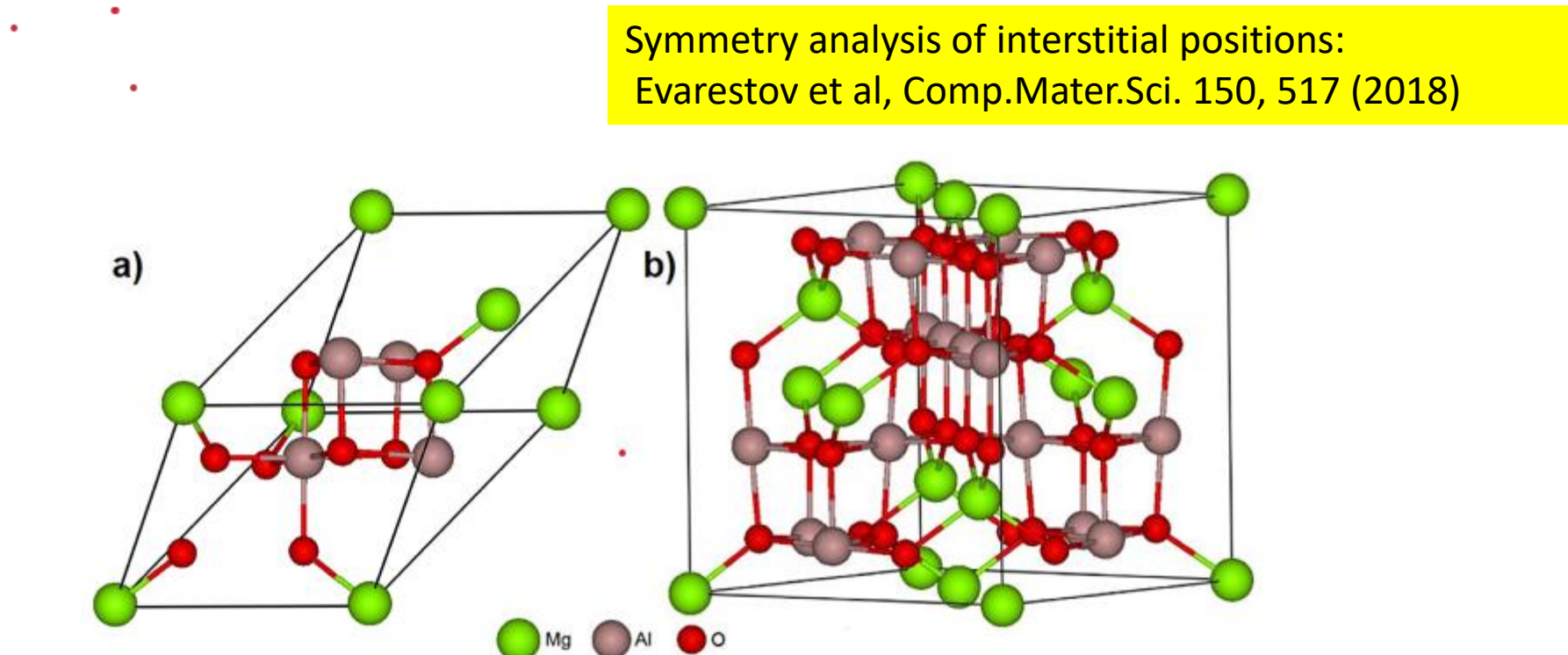
Bulk properties (test)

Properties	Expt.	LCAO-B3PW-CRYSTAL-14
Cell parameter, Å	a = 8.06	a = 8.037
Band Gap, eV	~7.8	8.79
Bulk modulus, GPa	198	212
c ₄₄ , GPa	155	161
Infra-red active frequencies, cm ⁻¹	304-312, 476-610, 578, 676-868	308, 503, 608, 711 (all F1u)



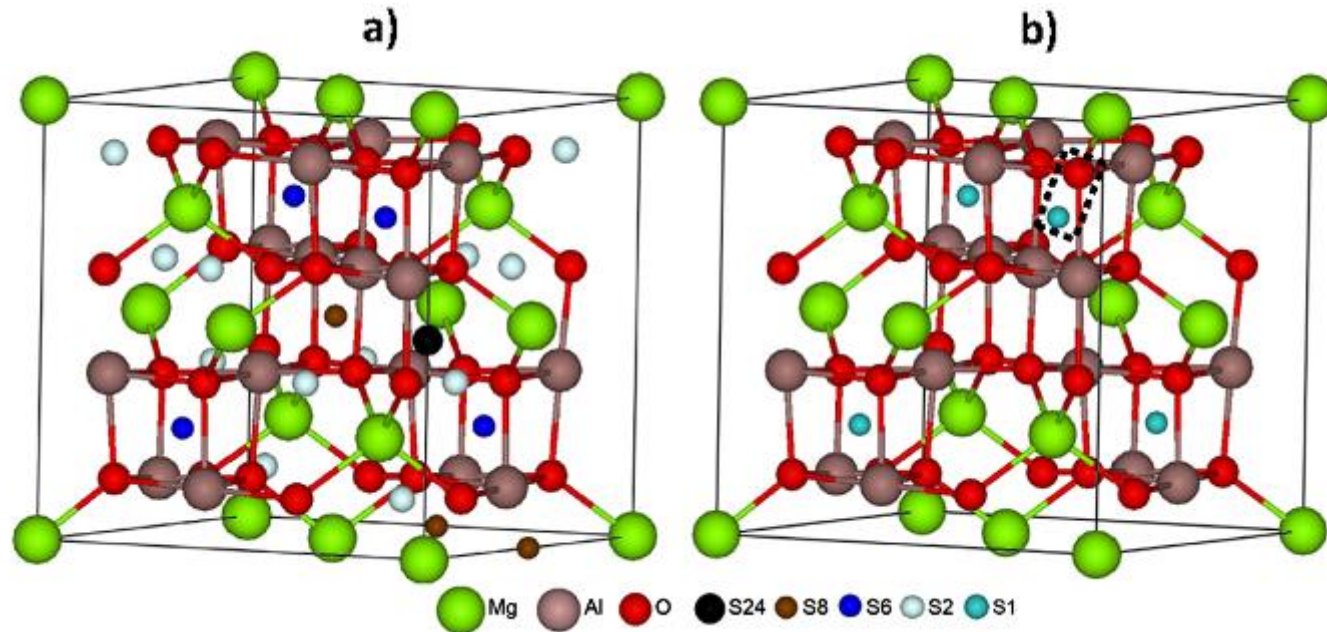
Evarestov et al, Comp. Mater. Sci. 150, 517 (2018)
Considerable covalency: q(O) = -1.13e,
q(Al) = 1.44e, q(Mg) = 1.63 e

Rhombohedral 14-atom unit cell and cubic-type 56-atom cell of MgAl₂O₄ spinel (SG 227)



New feature: anti-side defects

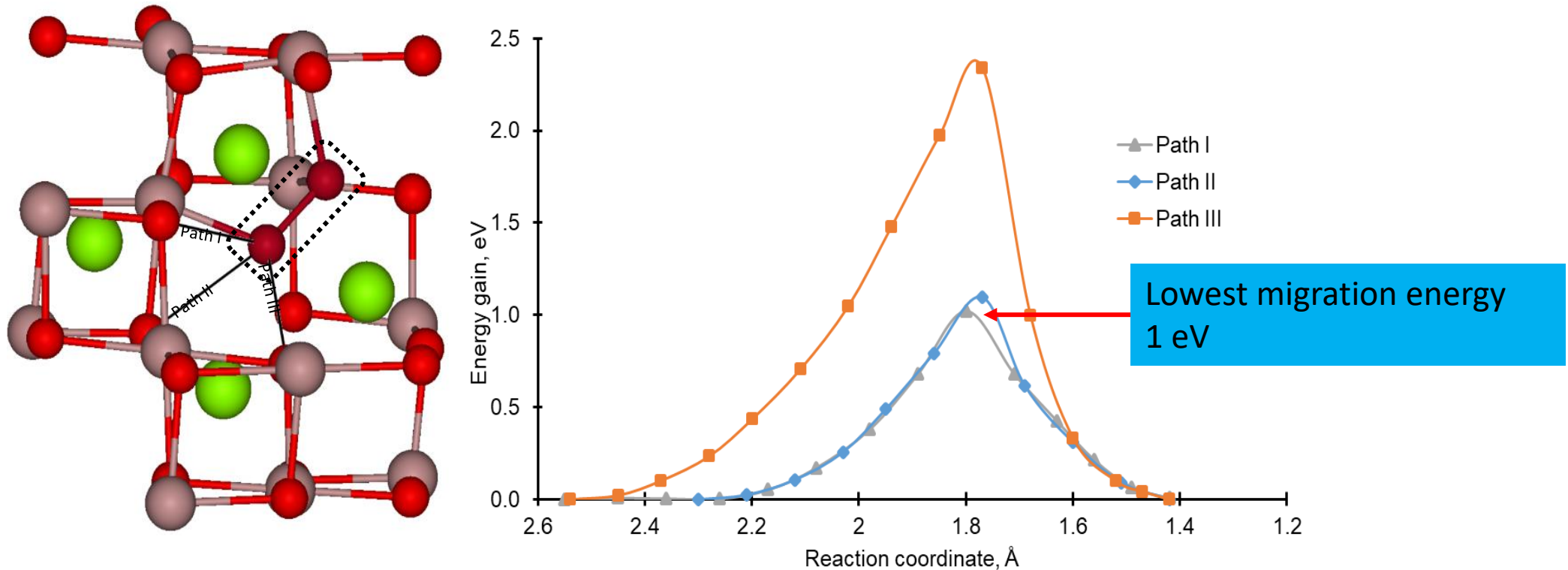
Five types of interstitial positions



Dumbbell formation ($d=1.43$ Å), vibrations 1142 cm $^{-1}$

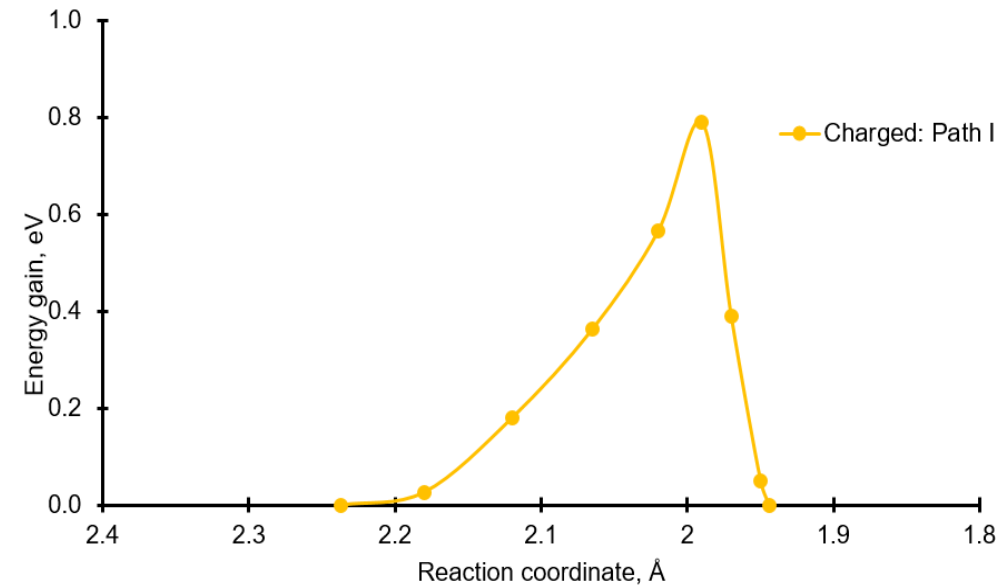
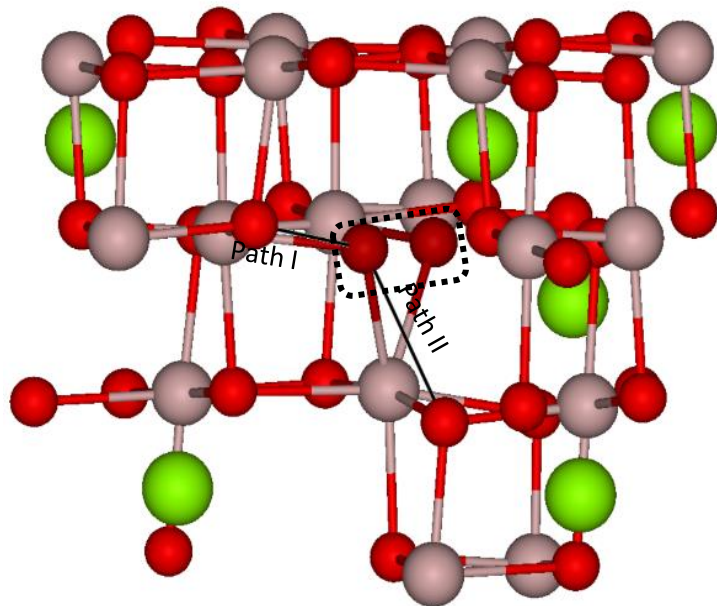
Migration of neutral oxygen interstitials in spinel: 3 possible paths

Platonenko et al, phys stat sol B 256, 1800282 (2018)



Left: fragment of 113 atom supercell with three migration paths of neutral O_i in spinel crystal. Green balls correspond to Mg atoms, grey-brown – Al atoms, and red – O atoms. The dumbbell ($O-O$ pair) is shown in dark red and highlighted with dotted rectangle. Right: the energy curves for three migration paths of neutral O_i with d energy barriers. The reaction coordinate is the distance between end atom of a dumbbell and a regular O ion to which it moves

Migration of charged interstitials



Left: fragment of 113 atom supercell with two migration paths of charged O_i in spinel crystal. O-O pair atoms shown in dark red and highlighted with dotted rectangle.
Right: Energy curves for migration paths of charged O_i with estimated energy barriers.

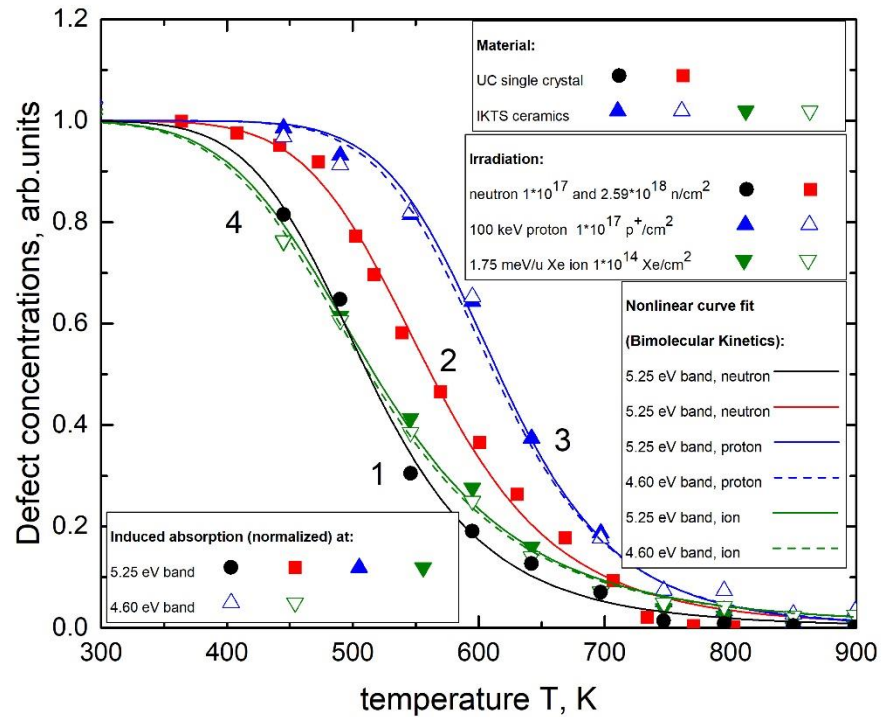
Migration energy of charged oxygen interstitial (0.8 eV) is smaller than for a neutral one (1eV)
Interstitials tend to form dumbbells (split interstitials)

Dumbbell properties in MgAl₂O₄ spinel -- classification by 3 properties:

1. O-O bond length: 1.42 Å (neutral Oi); 1.95 Å (O-)
-- Superoxide O₂(-) 1.33 Å; peroxide O₂ (2-) 1.49 Å
2. Total charge: -1.26 e (neutral Oi); -2.5 e (O-)
3. Stretching vibrational frequency: 1142 cm⁻¹ (neutral Oi),
Superoxide 1145 cm⁻¹
no such mode for a charged O-

Experimental proof needed: Raman? Kinetics?

MgAl₂O₄ spinel (Lushchik et al, Scientif Reports 10, 7810 (2020))



Good fit of data for both single crystals and ceramics, as well as different irradiations: universal law!

-- **No clean correlation** with hole defect annealing (O- bound to vacancies or anti-sites) → several step recombination process, instead of bimolecular recombination F+H=0

Disagreement with calculations for Oi:

Platonenko et al, PSS B, **256**, 1800282 (2019)

The obtained effective migration energies E_a (eV) and pre-exponential factors X (K⁻¹). Numbers in brackets correspond to the curves 1-4.

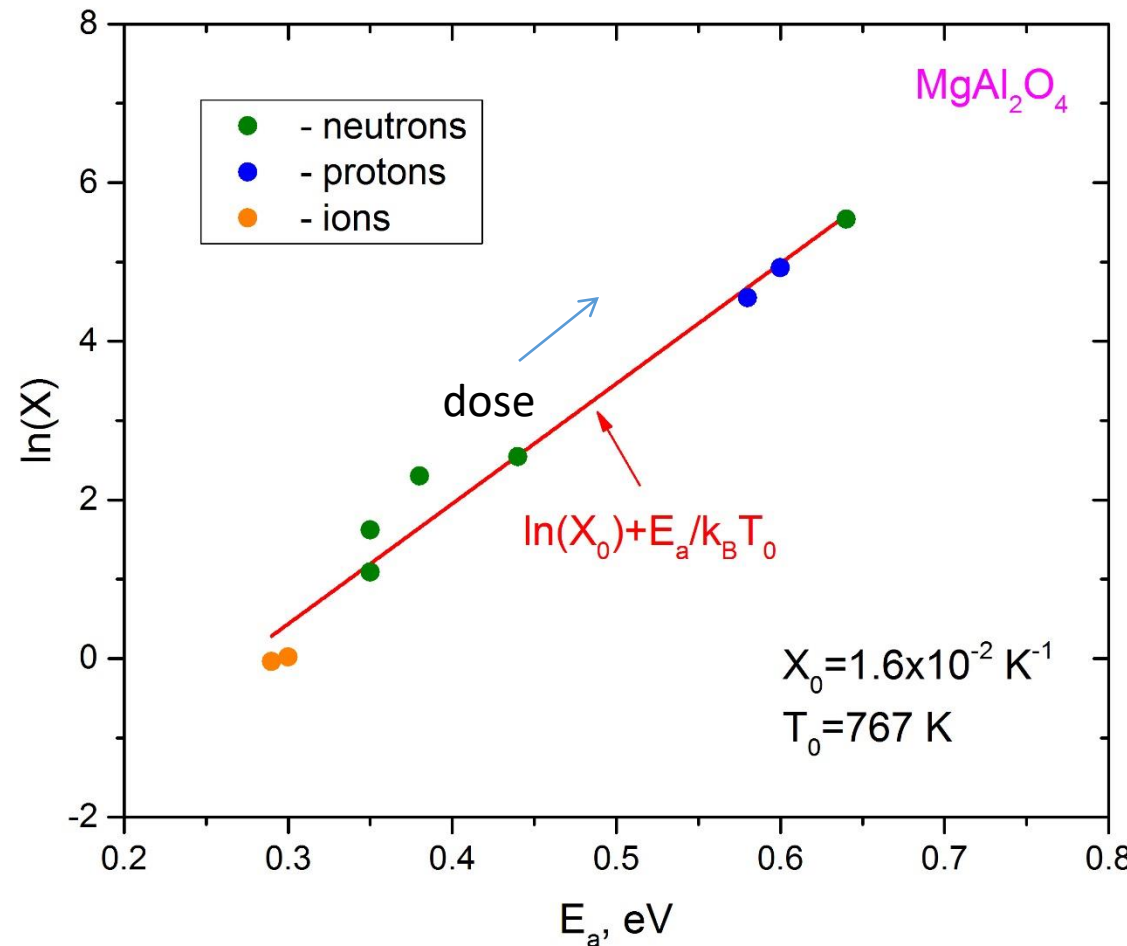
F-bands:	Ions, ceramics (4)	Neutrons, single crystal (1)	Neutrons, single crystal (2)	Protons, ceramics (3)
5.25 eV	$0.30, 1.02 \times 10^0$	$0.38, 9.96 \times 10^0$	$0.44, 1.27 \times 10^1$	$0.60, 1.38 \times 10^2$
4.60 eV	$0.29, 9.66 \times 10^{-1}$			$0.58, 9.43 \times 10^1$

Table 1. Explanation of curves I-V in Fig. 3 and the values of calculated migration energy E_a and pre-exponential factor X obtained under different irradiation conditions for the electron (Nos.1-12) and hole (Nos. 13 and 14) centers.

No.	Irradiation	Defect	E_a (eV)	$X(K^{-1})$	Legend
1 (I)	neutron	F	0.38	1.0×10^1	Optical absorption, single crystal, 1 MeV, $\Phi = 1.0 \times 10^{17} n/cm^2$
2	neutron	F^+	0.35	5.1×10^0	same as No. 1
3 (II)	neutron	F	0.44	1.3×10^1	Optical absorption, single crystal, 1 MeV, $\Phi = 2.6 \times 10^{18} n/cm^2$,
4	neutron	F^+	0.35	3.0×10^0	same as No. 3
5 (III)	protons	F	0.60	1.4×10^2	Optical absorption, ceramics with grain size 12 μm , 100 keV, $\Phi = 1.0 \times 10^{17} p/cm^2$
6	protons	F^+	0.58	9.4×10^1	same as No. 5
7 (IV)	proton	F	0.24	8.5×10^{-2}	Optical absorption, ceramics with grain size 1.4 μm , 100 keV, $\Phi = 1.0 \times 10^{17} p/cm^2$
8	proton	F^+	0.24	8.7×10^{-2}	same as No. 7
9	proton	F	0.29	3.4×10^{-1}	Optical absorption, ceramics with grain size 1.4 μm , 100 keV, $\Phi = 5.0 \times 10^{17} p/cm^2$
10	proton	F^+	0.22	9.3×10^{-2}	same as No 9
11	proton	F	0.34	1.1×10^0	Optical absorption, ceramics, grain size 0.5 μm , 100 keV, $\Phi = 2.0 \times 10^{17} p/cm^2$
12	proton	F^+	0.38	3.1×10^0	same as No. 11
13 (V)	neutron	V_2	0.64	2.5×10^2	EPR signal, single crystal 1 MeV, $\Phi = 2.6 \times 10^{18} n/cm^2$
14	neutron	V_1	0.63	1.9×10^5	same as No. 13

Inverse dose dependence!

Critical role of
anti-site defects
In Oi migration?



Hole centers in spinel: Platonenko et al, NIM B 464, 60 (2020)

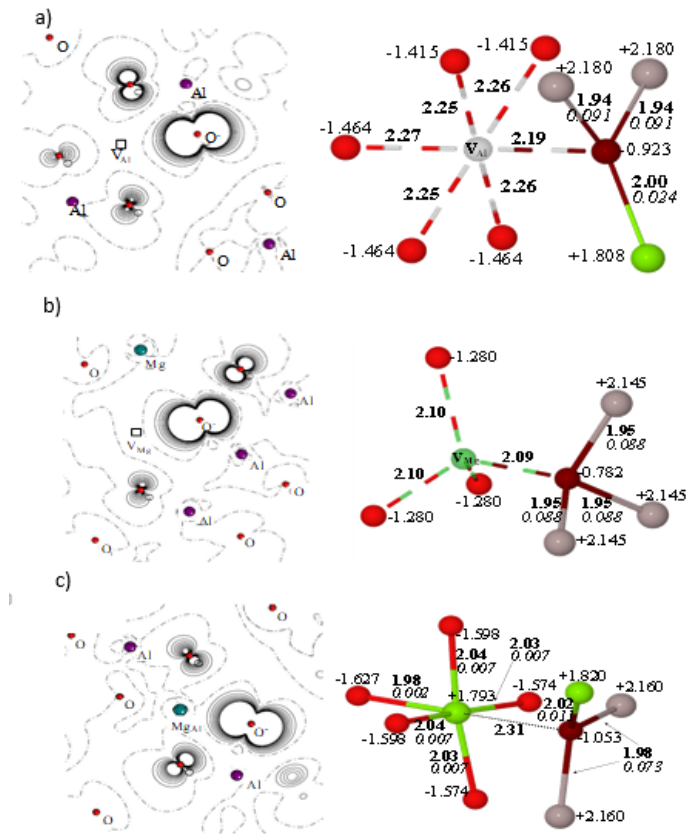


Fig. 1. 2D spin density maps (left) for V_1^- (a), V_2^- (b), V_{22}^- (c) centres and corresponding atomic relaxation patterns (right) around O^- defects. On right: red balls O ions, gray balls Al ions, green balls Mg ions and anti-site, dark red ball O^- , light gray ball Al vacancy (a), dark green ball Mg vacancy (b). There is an effective atomic charge in e for each ion on right whereas the numbers marked in bold show inter-atomic distances in Å.

Calculations of three types of hole paramagnetic centers in $MgAlO_4$ spinel:

V_1 : O^- trapped by Al vacancy

V_2 : O^- trapped by Mg vacancy

V_{22} : O^- trapped by antisite (Mg vs Al)

Atomic, electronic, magnetic structure and hyperfine coupling constants were calculated

Defect	Q/e	M/μ_B
V_1	-0.92	0.78
V_2	-0.78	0.80
V_{22}	-1.05	0.72

Defect recombination kinetics in irradiated MgAl_2O_4

Table 1. The obtained effective migration energies E_a (eV) and pre-exponential factors X (K^{-1}) .
Numbers in brackets correspond to the curves 1-4 in fig.1.

F-bands:	Ions, ceramics (4)	Neutrons, single crystal (1)	Neutrons, single crystal (2)	Protons, ceramics (3)
5.25 eV	0.30, 1.02x10 ⁰	0.38, 9.96x10 ⁰	0.44, 1.27x10 ¹	0.60, 1.38x10 ²
4.60 eV	0.29, 9.66x10 ⁻¹			0.58, 9.43x10 ¹

Table 2. The activation energy and preexponential factors for V1 and V2 centers.

EPR	V ₁ center	V ₂ center
	0.63, 1.9x10 ⁵	0.64, 2.5x10 ²

A comparison of parameters obtained for the V₂ and F centers for the same neutron fluencies ($2.59 \cdot 10^{18} \text{ cm}^{-2}$) shows that the activation energy for the former defects (0.64 eV) is larger than that for the F center (0.44 eV) whereas the pre-exponential factors are qualitatively similar.

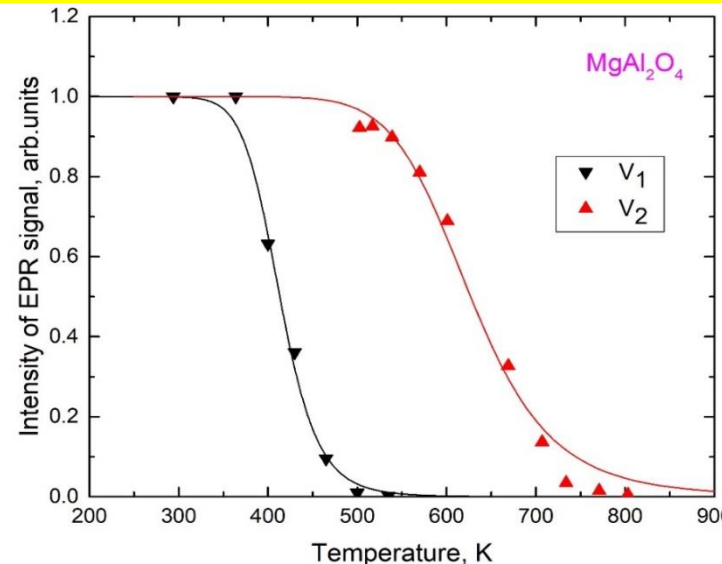
This indicates that the recombination process is quite complicated and probably involves several times of hole centers, all contributing to the F annealing.

On the other hand, the parameters of the V₂ center fit very well to the MNR curve confirming F-V correlated recombination.

This is in contrast with the V₁ center (table shows very (3 orders of magnitude) larger preexponential factor than that for the V₂ center, its position fall well far away from the MNR curves.

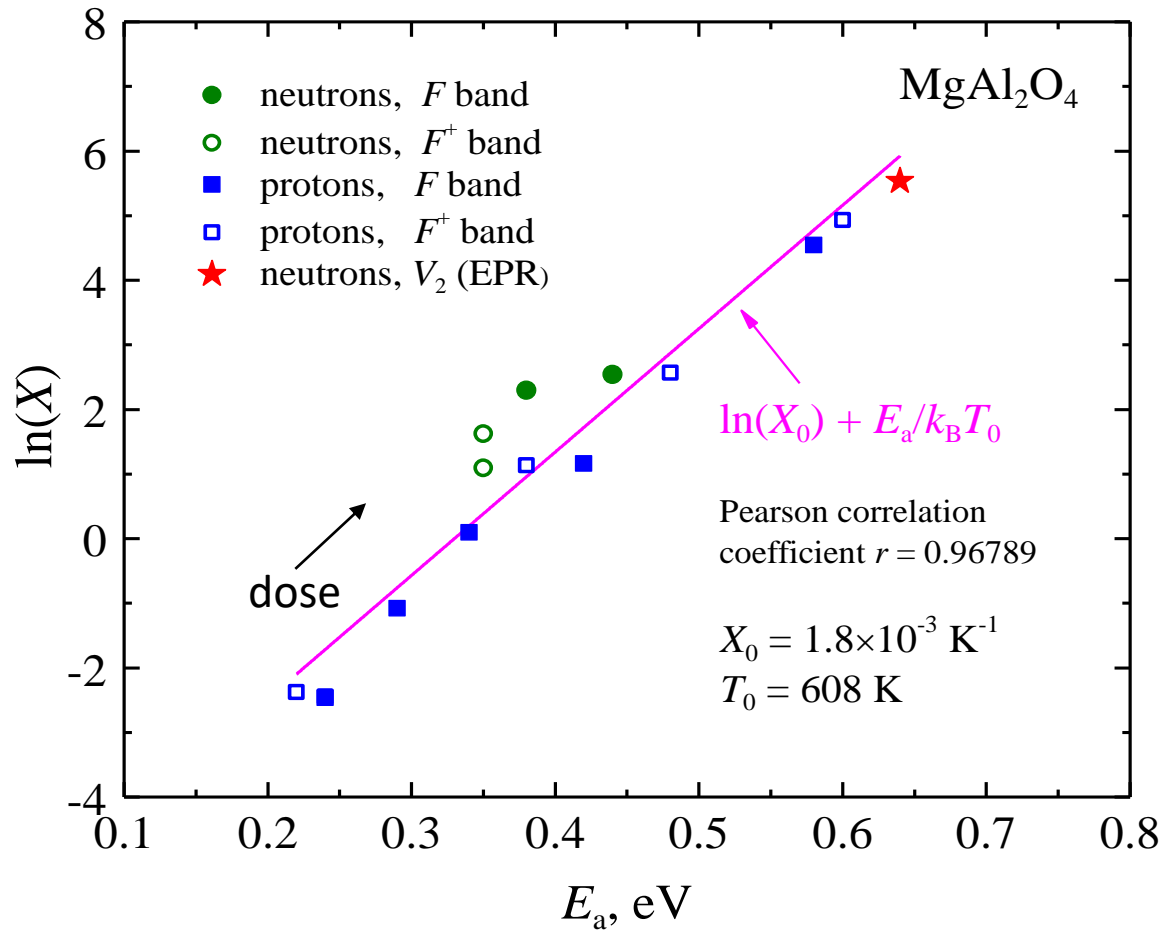
Such large preexponential factor indicates at the electronic process when defects are not migrating but likely holes are delocalized from traps, move through the valence band and recombine with the F centers.

Lushchik et al, Scientific Reports 10, 7810 (2020)



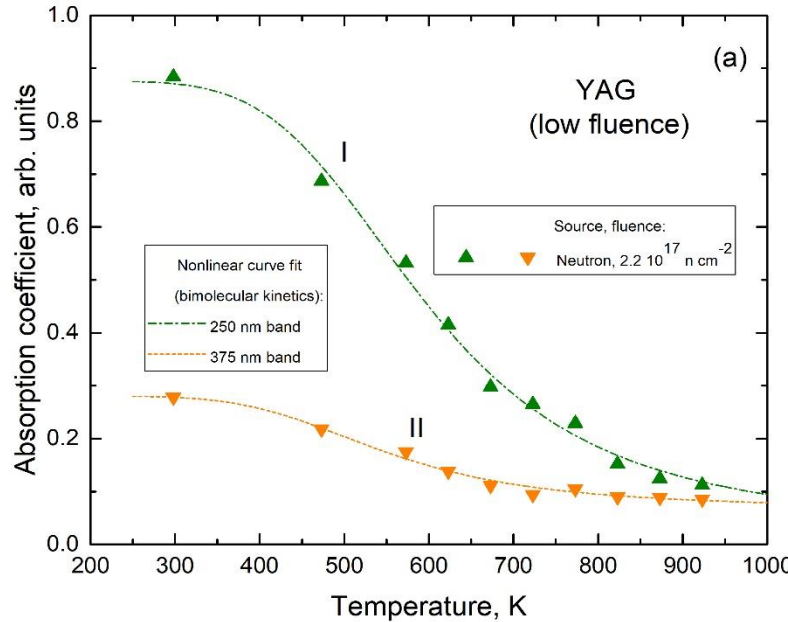
Inverse dose dependence!

Critical role of
Anti-site defects
In Oi migration?



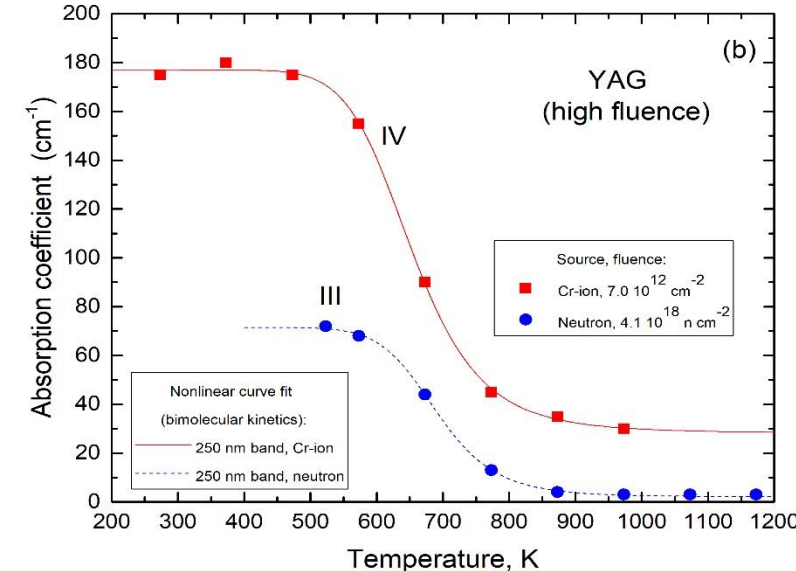
The last example: $\text{Y}_3\text{Al}_5\text{O}_{12}$ (YAG)

(M.Izerrouken, *heavy ions and reactor neutrons*)



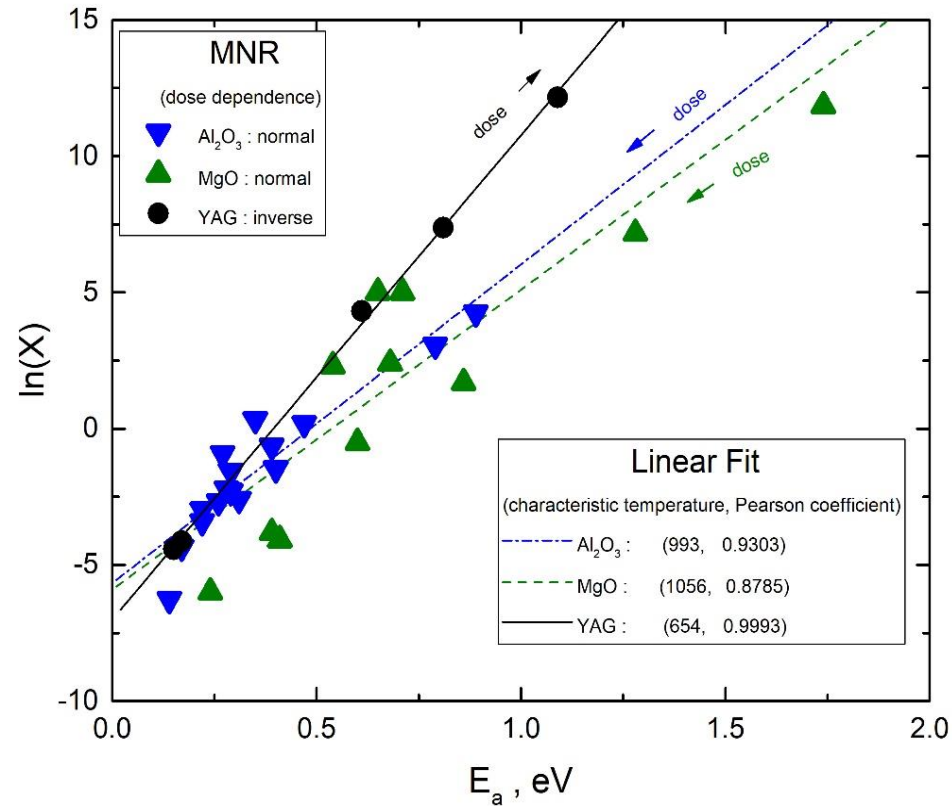
The annealing kinetics of the F-type centers in YAG (Izerrouken et al, NIM B (2007)), after low (a) and high (b) radiation fluencies.
Symbols are experimental data, lines is theoretical modelling.

Good fit of data for different irradiations.



Inverse dose dependence!

The Meyer-Neldel rule for YAG (this study) as well as Al_2O_3 and MgO (Kotomin et al, J. Phys Chem A (2018)). Directions of the radiation fluence (dose) increase are shown by arrows.



Conclusions

- Radiation- induced interstitial oxygen ions form dumbbells, which confirmed experimentally in corundum
- In strongly irradiated ionic solids radiation defect migration is not necessarily characterized by unique migration energy with constant pre-exponent!
- This makes data analysis quite complicated
- radiation fluences play an important role
- local disoreding of the crystalline structure?
- defect cluster formation at high doses?

The presented results could be understood as a growing topological disordering of materials under irradiation with a continuous transition from a perfect crystalline structure to the amorphous-like one.

This could explain drastic reduction of the activation energy for diffusion. As is known, in liquids the main migration mechanism is not thermally activated overcome of the energy barrier between two lattice positions, but particle (molecule) penetration into nearest cavity due to density fluctuation when nearest molecules are collectively move apart opening the path for a random walk with a low activation energy.

The characteristic feature of liquids and amorphous solids is a strong temperature dependence of the pre-exponential factor which is **no** longer a constant.

Recent publications (2018-2020)

- 1) **V.N. Kuzovkov, E.A. Kotomin, and A.I. Popov.**
Kinetics of dimer F₂ type center annealing in MgF₂ crystals.-- *Nucl. Instrum. Methods Phys. Res. B*, 2018, **435**, pp. 79–82.
- 2) **A. Platonenko, D. Gryaznov, Yu.F. Zhukovskii, and E.A. Kotomin.**
Ab initio simulations on charged interstitial oxygen migration in corundum. -- *Nucl. Instrum. Methods Phys. Res. B*, 2018, **435**, pp. 74–78.
- 3) A. Lushchik, S. Dolgov, E. Feldbach, R. Pareja, **A.I. Popov**, E. Shablonin, and V. Seeman.
Creation and thermal annealing of structural defects in neutron-irradiated MgAl₂O₄ single crystals.--*Nucl. Instrum. Methods Phys. Res. B*, 2018, **435**, 31–37.
- 4) **A. Platonenko, D. Gryaznov, Yu.F. Zhukovskii, and E.A. Kotomin.**
First principles simulations on migration paths of oxygen interstitials in MgAl₂O₄.-- *Phys. Status Solidi B*, 2018, **255**, 1800282 (pp. 1-7).
- 5) **A.I. Popov, A. Lushchik, E. Shablonin, E. Vasil'chenko, E.A. Kotomin, A.M. Moskina, and V.N. Kuzovkov.**
Comparison of the F-type center thermal annealing in heavy-ion and neutron irradiated Al₂O₃ single crystals.--*Nucl. Instrum. Methods Phys. Res. B*, 2018, **433**, pp. 93-97.
- 6) **V.N. Kuzovkov, E.A. Kotomin, and A.I. Popov.**
Kinetics of the electronic center annealing in Al₂O₃ crystals.-- *J. Nucl. Mater.*, 2018, **502**, pp. 295-300.
- 7) **E. Kotomin, V. Kuzovkov, A.I. Popov, J. Maier, and R. Vila.**
Anomalous kinetics of diffusion-controlled defect annealing in irradiated ionic solids.-- *J. Phys. Chem. A*, 2018, **122**, pp. 28–32.
- 8) **A. Platonenko, D. Gryaznov, Yu.F. Zhukovskii, E.A. Kotomin.**
First principles simulations on migration paths of oxygen interstitials in MgAl₂O₄.-- *Phys. Status Solidi B*, 2019, **256**, 1800282 (pp. 1-7).
- 9) **A. Platonenko, D. Gryaznov, E.A. Kotomin, A. Lushchik, V. Seeman, A.I. Popov.**
Hybrid density functional calculations of hyperfine coupling tensor for hole-type defects in MgAl₂O₄.--*Nucl. Instrum. Methods Phys. Res. B*, 2020, **464**, pp. 60–64.
- 10) G. Baubekova, A. Akilbekov, **E.A. Kotomin, V.N. Kuzovkov, A.I. Popov**, E. Shablonin, E. Vasil'chenko, M. Zdorovets, A. Lushchik.
Thermal annealing of radiation damage produced by swift ¹³²Xe ions in MgO single crystals.-- *Nucl. Instrum. Methods Phys. Res. B*, 2020, **462**, pp. 163–168.
- 11) V.Seeman, A. Lushchik, E.Shablonin, **D.Gryaznov, A. Platonenko, E.A. Kotomin, A.I.Popov et al**, Scientific Reports, 2020, in press
- 12) A.Lushchik, E.Feldbach, E.A. Kotomin, V.N.Kuzovkov, A.I.Popov et al, Scientific Reports, 2020, 10, 7810.

Many thanks to
Yu. Zhukovskii (Riga, died 2019)
V. Lisitsyn (Tomsk)
A. Lushchik (Tartu, Estonia)
R.Evarestov (St.Petersburg),
and you for attention!